



Symmetric Atom–Atom and Ion–Atom Processes in Stellar Atmospheres

Vladimir A. Srećković ^{1,*} , Ljubinko M. Ignjatović ¹ and Milan S. Dimitrijević ^{2,3} 

¹ Institute of Physics, University of Belgrade, Pregrevica 118, Zemun, 11080 Belgrade, Serbia; ljuba@ipb.ac.rs

² Astronomical Observatory, Volgina 7, 11060 Belgrade, Serbia; mdimitrijevic@aob.rs

³ LERMA, Observatoire de Paris, UMR CNRS 8112, UPMC, 92195 Meudon CEDEX, France

* Correspondence: vlada@ipb.ac.rs

Received: 7 September 2017; Accepted: 19 December 2017; Published: 21 December 2017

Abstract: We present the results of the influence of two groups of collisional processes (atom–atom and ion–atom) on the optical and kinetic properties of weakly ionized stellar atmospheres layers. The first type includes radiative processes of the photodissociation/association and radiative charge exchange, the second one the chemi-ionisation/recombination processes with participation of only hydrogen and helium atoms and ions. The quantitative estimation of the rate coefficients of the mentioned processes were made. The effect of the radiative processes is estimated by comparing their intensities with those of the known concurrent processes in application to the solar photosphere and to the photospheres of DB white dwarfs. The investigated chemi-ionisation/recombination processes are considered from the viewpoint of their influence on the populations of the excited states of the hydrogen atom (the Sun and an M-type red dwarf) and helium atom (DB white dwarfs). The effect of these processes on the populations of the excited states of the hydrogen atom has been studied using the general stellar atmosphere code, which generates the model. The presented results demonstrate the undoubted influence of the considered radiative and chemi-ionisation/recombination processes on the optical properties and on the kinetics of the weakly ionized layers in stellar atmospheres.

Keywords: atomic processes; molecular processes; radiative transfer; absorption quasi-molecular bands; sun:atmosphere; sun:photosphere; stars:atmospheres; white dwarfs

1. Introduction

Atomic and molecular data play a key role in many areas of science like atomic and molecular physics, astrophysics, nuclear physics, industry, etc. [1–9]. The interpretation of interstellar line spectra with radiative transfer calculations usually requires spectroscopic data and collision data (e.g., atomic parameters, cross sections, etc.) [10,11]. Determination of accurate fundamental stellar parameters is one of the most important of today's tasks and this area of fundamental science is very important and still current. For example, the atomic and molecular data are important for development of atmosphere models of solar and near solar type stars and for radiative transport investigations as well as an understanding of the kinetics of stellar and other astrophysical plasmas [12]. Available LTE codes for stellar atmosphere modelling like ATLAS [13,14], MARCS [15] as well as NLTE codes like e.g., PHOENIX (see e.g., [16,17]) and TLUSTY [18,19] require the knowledge of atomic and molecular data. In addition, spectrum synthesis codes (e.g., SYNTHE, SYNSPEC) for radiative transfer and spectra depend on these as input parameters [20]. Such atomic data and processes are also important in modelling early Universe chemistry (see [21]). Evaluation of chemical abundances in the standard Big Bang model are calculated from a set of chemical reactions for the early universe and among them are very important reactions with species like H, H₂⁺ and also different Rydberg atoms [22]. The highly excited atomic states are named 'Rydberg states', and the atoms in such states are called

‘Rydberg atoms’. Strictly speaking, only highly excited states, should be counted among the Rydberg states. However, in practice, an atom $A^*(n, l)$ is being treated as a Rydberg atom if $(n - n_0) \geq 4$, where n_0 is the principal quantum number of the outer shell of the atom A in its ground state, and in the case of an atom $\text{He}^*(n)$ —for any $n \geq 3$. It should be noted that, at the present time, even in the laboratory experiments, Rydberg atoms with n close to 10^2 are being explored, while the astrophysicists observe the radiation of atoms from the states with n close to 10^3 . With a change of n , the parameters characterizing Rydberg states may change by orders of magnitude.

The content of this article is distributed in four sections. The first is devoted to the detailed description of the processes, and the corresponding methods of the determination of such processes coefficients and parameters. Sections 2 and 3 show the existing theoretical results concerning the investigated processes, their role in the low temperature layers of stellar atmospheres, as well as the methods of the investigation of such processes. Finally, at the end of this article, the current research and directions of further research are summarized.

In a series of papers [23–27], two groups of atom–Rydberg atom and ion–atom collisional processes have been studied from the point of view of their effect on the optical and kinetic properties of weakly ionized laboratory and astrophysical plasmas.

The first group of them includes chemi-ionization and chemi-recombination processes of the type



where $A^*(n)$ is an atom in a highly excited (Rydberg) state with a principal quantum number $n \gg 1$, and e is a free electron. The processes caused by the action of the resonant energy exchange mechanism inside the electron component corresponding to the atomic–atomic or electron–ion–atomic system are considered [28]. These processes are illustrated in the Figure 1, where Figure 1a schematically shows the geometry of the collision $A^*(n) + A$, and Figure 1b—the essence of the resonant mechanism is that the transition of an external weakly bound electron of the system (e_n) with energy $\varepsilon_n < 0$ to a free state with energy $\varepsilon_k > 0$ is accompanied by a transition of the subsystem $A + A^+$ from the first excited molecular state with energy $U_2(R)$ to the ground state with energy $U_1(R)$.

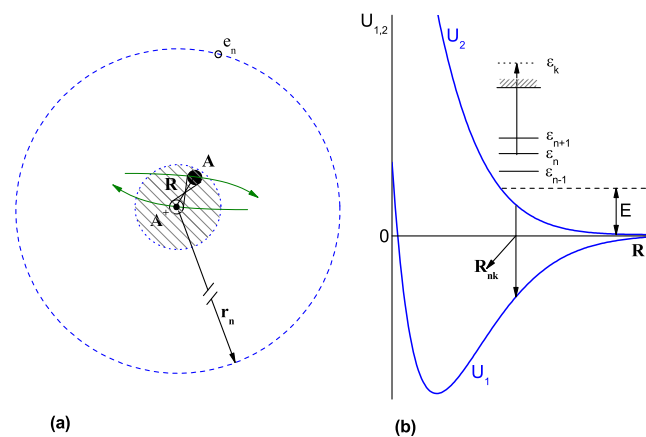
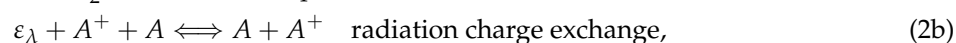


Figure 1. (a) schematic illustration of $A^*(n, l) + A$ collision (1) within the domain of internuclear distances $R \ll r_n$, where r_n is the characteristic radius of Rydberg atom $A^*(n, l)$; (b) schematic illustration of the resonance mechanism.

The second group of processes includes radiation processes of the type:



where ε_{λ} stands for the energy of a photon with a wavelength λ , A and A^+ —an atom and its positive ion in the ground states, and A_2^+ —a molecular ion in the ground electronic state. These processes are illustrated in the Figure 2, where $U_1(R)$ and $U_2(R)$ represent the adiabatic potential curves of the ground and first excited electronic state of the ion, and R stands for the internuclear distance in atomic units. This figure shows that the radiative processes under study represent the result of transitions, with the emission or absorption of a photon, between the mentioned molecular electronic states.

The effect of chemi-ionization and chemi-recombination processes (1) can be estimated by comparing their intensities with the intensities of known concurrent ionization and recombination processes, namely:

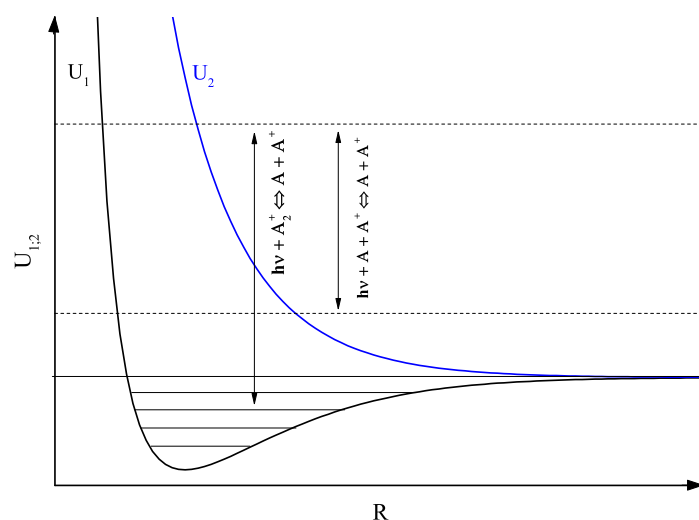


Figure 2. The schematic presentation of the photo-dissociation/association processes Equation (2a) and free-free processes Equation (2b): R is the internuclear distance, $U_1(R)$ and $U_2(R)$ are the potential energy curves of the initial (lower) and final (upper) electronic state of molecular ion A_2^+ , and $h\nu$ is the photon energy.

The influence of radiation processes (2) can be analysed by comparing with the intensities of known concurrent radiative processes, namely:



where A^- is stable negative ion.

In connection with astrophysical plasmas, two cases are considered:

- the case of hydrogen, when $A = \text{H}(1s)$ and $A^+ = \text{H}^+$,
- the case of helium, when $A = \text{He}(1s^2)$ and $A^+ = \text{He}^+(1s)$.

For the solar atmosphere, A usually denotes atom $\text{H}(1s)$ and $A^+ = \text{H}^+$, and, for the case of helium-rich white dwarf atmospheres, A denotes $\text{He}(1s^2)$ and $A^+ = \text{He}^+(1s)$.

Chemi-ionization/recombination processes are very important for the evolution of Universe in the early epochs. The most important process is hydrogen recombination, and Rydberg states can play important roles in this process [22].

2. Chemi-Ionization and Chemi-Recombination Processes

The region of importance of chemi-ionization processes and production of Rydberg atoms i.e., chemi-recombination is in the cool dwarf stars and, especially, cool white dwarfs. Spectroscopic observations of cool white dwarfs [29] have demonstrated that white dwarfs with temperatures less than 6100 K are found to display significant flux deficits that are not predicted by the current WD model. One can suggest that such process may be absorption by atoms and molecules in highly excited Rydberg states.

Recent research of the atmospheres of cooling stars such as white dwarfs pointed out an anomaly in light emission of Rydberg atom with $n = 10$ and tabular lifetime $\tau \sim 10^{-6}$ s. The lines of the corresponding infra-red transitions have not been observed [30]. Let us note that it is just these states that correspond to the maximal values of chemi-ionization rate coefficients. According to the observational data, we have that, under such conditions $N_0 \geq 10^{17} \text{ cm}^{-3}$ and $N^* \geq 10^{13} \text{ cm}^{-3}$, where N_0 and N^* are the densities of the ground state and Rydberg atoms. It is not difficult to estimate that the probability of a Rydberg atom being extinguished through the chemi-ionization channel is comparable to the probability of its radiative decay.

Let us not forget the importance of chemi-ionization processes and production of Rydberg atoms in chemistry, physics and related branches of science [28,31,32].

In this article, the current state of research of the processes in atom–Rydberg atom collisions is presented. The principal assumptions of the model of such processes are based on the dipole resonance mechanism.

The chemi-ionization and inverse chemi-recombination processes (1) can be considered from the point of view of their effect on the population of the excited states of the hydrogen atoms in solar and cold-star atmospheres, as well as on the population of excited states of the helium atoms in DB white dwarfs. Comparative analysis of the influence of these and concurrent processes (3) and (4) can be presented by the values of the following parameters:

$$F_{phr}^{(ab)}(2,8) = \frac{\sum_{n=2}^8 I_r^{(ab)}(n,T)}{\sum_{n=2}^8 I_{phr}^{(ab)}(n,T)}, \quad F_{eei}^{(ab)}(2,8) = \frac{\sum_{n=2}^8 I_r^{(ab)}(n,T)}{\sum_{n=2}^8 I_r^{(eei)}(n,T)}, \quad F_i(n,T) = \frac{I_{ci}(n,T)}{I_{i;ea}(n,T)}, \quad (8)$$

where $I_{ci}(n,T)$, $I_{i;ea}(n,T)$, $I_r^{(ab)}(n,T)$, $I_{phr}^{(ab)}(n,T)$ and $I_r^{(eei)}(n,T)$ are the fluxes caused by ionization and recombination processes (1), (3) and (4).

2.1. Solar Atmosphere

As a necessary step to improve the modeling of the solar photosphere, as well as to model atmospheres of other similar and cooler stars where the main constituent is also hydrogen, it is required to take into account the influence of all the relevant collisional processes on the excited-atom populations in weakly ionized hydrogen plasmas. This is important since a strong connection between the changes in atom excited-state populations and the electron density exists in weakly ionized plasmas.

It is a fact that, with an increase of the electron density, caused by a growth of the excited hydrogen atom population, the rate of thermalization by electron–atom collisions in the stellar atmosphere will become higher. A consequence will be that the radiative source function of the line center will be more closely coupled to the Planck function, making the synthesized spectral lines stronger for a given model structure, affecting the accuracy of plasma diagnostics and determination of the atmospheric pressure.

The theoretical investigation of the processes (1) started in [33] for the hydrogen symmetric case $A = H$. Although some of the chemi-ionization processes in atom–Rydberg atom collisions had already been described in [33], their intensive astrophysical research began somewhat later. From the astrophysical point of view, in Ref. [34], an investigation was started for the chemi-recombination processes of the photosphere and the lower chromosphere of the Sun, where $4 \leq n \leq 8$. Further research of Mihajlov and coworkers continued in [35] on the chemi-ionisation processes in $H^*(n \geq 2) + H(1s)$ collisions and inverse recombination in the photosphere and the lower chromosphere of the Sun.

The partial rate coefficients for the chemi-ionization processes (1a,b) are determined by expressions

$$K_{ci}^{(a,b)}(n, T) = \int_{E_{min}(n)}^{\infty} v \sigma_{ci}^{(a,b)}(n, E) f(v; T) dv, \quad (9)$$

where $\sigma_{ci}^{(a,b)}(n, E)$ is cross section, v is the atom–Rydberg–atom impact velocity, $f(v; T)$ is the velocity distribution function for the given temperature T , and $E_{min}(n)$ is determined by the behavior of the potential curve $U_2(R)$ and the splitting term as presented in [35].

Under the conditions that exist in the solar atmosphere, the chemi-recombination rate coefficients can be presented over chemi-ionization rate coefficient

$$K_{ci}^{(a)}(n, T) \cdot N_n N_1 = K_{cr}^{(a)}(n, T) \cdot N_1 N_{ai} N_e, \quad (10)$$

where N_1 and N_n denote the densities of ground- and excited-state of atoms, respectively, while N_{ai} is the densities of ions.

Using partial rate coefficients $K_{ci,cr}^{(a,b)}(n, T)$, we can determine the total one,

$$K_{ci,cr}(n, T) = K_{ci,cr}^{(a)}(n, T) + K_{ci,cr}^{(b)}(n, T), \quad (11)$$

which characterizes the efficiency of the chemi-ionization/recombination processes (1a,b) together. The total chemi-ionization and chemi-recombination fluxes are $I_{ci}(n, T) = K_{ci}(n, T) \cdot N_n N_1$, $I_{cr}(n, T) = K_{cr}(n, T) \cdot N_1 N_i N_e$.

Figure 3a,b show the values of the total chemi-ionization and recombination rate coefficients $K_{ci}(n, T)$ and $K_{cr}(n, T)$ in the region $2 \leq n \leq 8$ and $5000 \text{ K} \leq T \leq 10,000 \text{ K}$ obtained in [35]. From the figure, it follows that the maximum values of the hydrogen $K_{ci}(n, T)$ lies at $n = 5$ for all temperatures (except for $T = 5000 \text{ K}$, where maximum value of $K_{ci}(n, T)$ are at $n = 4$), and maximum values for the chemi recombination rate coefficient $K_{cr}(n, T)$ shifts to higher n (from 3 to 5) when temperature increases. The relative importance of a particular channel ('a' and 'b') for the chemi-ionization and chemi-recombination processes (1a,b) is shown in Figure 4. Branch coefficient $X(n; T) = K_{ci,cr}^{(b)} / K_{ci}(n, T)$ present the ratio of rate coefficient for processes (1b) and total ((1a) + (1b)). From Figure 4, one can see that, for lower temperatures, i.e., 5000 K, processes (1b) are dominant while importance of processes (1a) increase with the increase of temperature as expected.

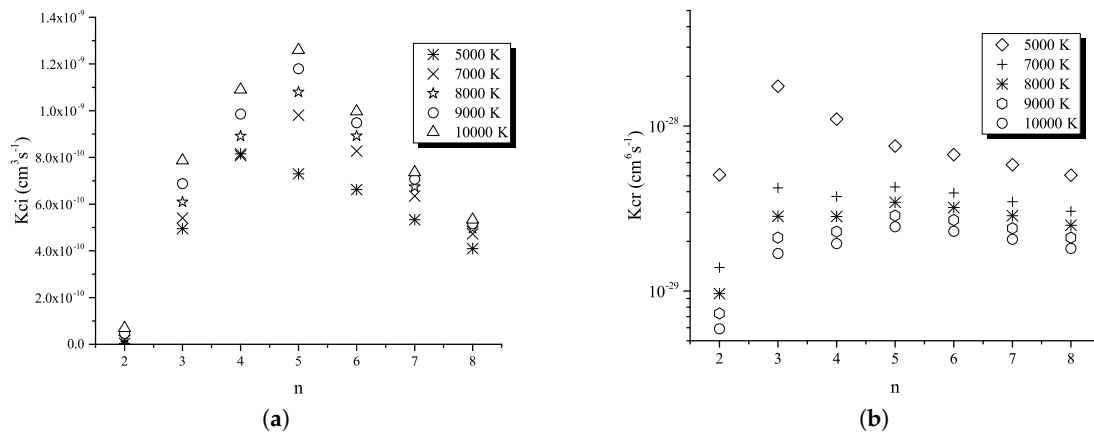


Figure 3. (a) total chemi-ionization rate coefficients $K_{ci}(n; T; H)$ with $5000 \text{ K} \leq T \leq 10,000 \text{ K}$ and for principal quantum numbers $n = 2$ – 10 ; (b) same as in (a) but for the inverse recombination coefficients $K_{cr}(n; T; H)$ (data taken from [35]).

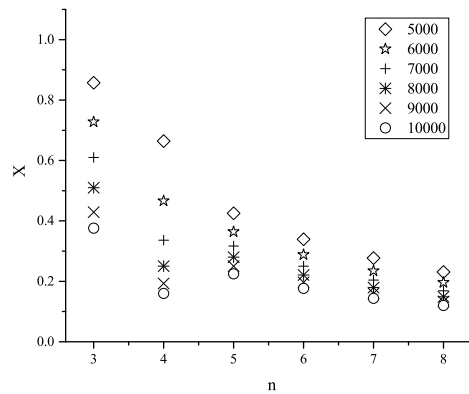


Figure 4. Same as in Figure 3 but for the branch coefficient $X(n; T; H)$, characterizing the relative importance of the particular channel ('a' and 'b') for the chemi-ionization and chemi-recombination processes (1a,b).

From the astrophysical point of view, the results have shown that, in some parts of the solar atmosphere, chemi-recombination processes (1) can dominate with respect to the photo-recombination process (3) and their intensity can be close to the intensity of triple electron–electron–ion recombination processes (4). The behavior of quantity $F_{phr}^{(ab)}$ as a function of h is shown in Figure 5a. The behavior of the quantity $F_{eei}^{(ab)}$ as a function of height h is shown in Figure 5b from [35]. One can see that the considered chemi-recombination processes dominate with respect to the concurrent electron–electron–ion recombination processes within the region $100 \text{ km} \leq h \leq 650 \text{ km}$ and significantly influence the optical properties of the solar photosphere. Namely, if we take the considered processes into account, we will improve the modeling of the solar photosphere, as the model atmospheres of other similar and cooler stars. If we do not take into account all relevant collisional processes on the excited-atom populations in weakly ionized plasmas, the corresponding electron density will be less accurate. For example, as stated in Reference [26], an increase of the electron density, caused by a growth of the excited hydrogen atom population, will result in a higher rate of thermalization by electron–atom collisions in the stellar atmosphere. As a consequence, the radiative source function of the line center will be more closely coupled to the Planck function, and the synthesized spectral lines will be stronger for a given model structure. This will influence on the accuracy of plasma diagnostics and determination of the atmospheric pressure.

Domination of the chemi-recombination processes with $2 \leq n \leq 8$ over the electron-ion photo-recombination processes is confirmed in a significant part of the photosphere ($-50 \text{ km} \leq h \leq 600 \text{ km}$). Thus, it is proofed that these processes are important for non-LTE modeling of solar atmosphere.

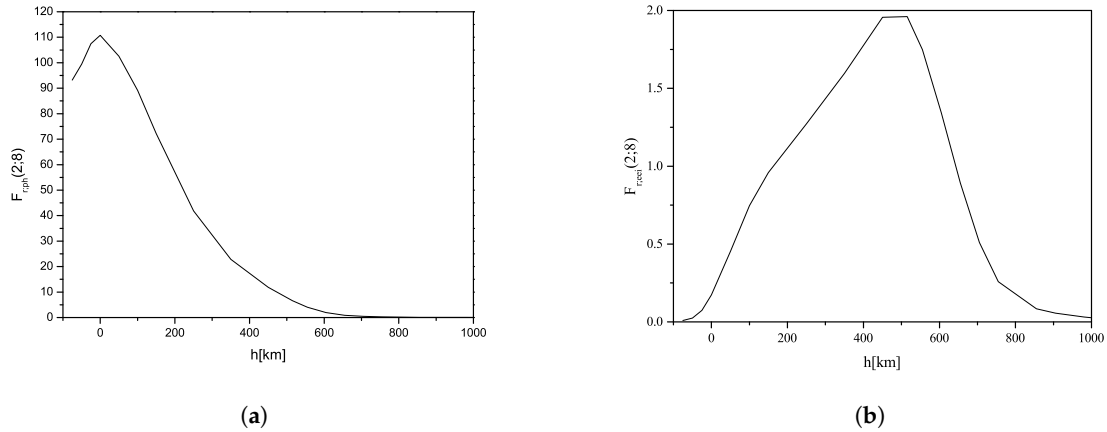


Figure 5. (a) parameter $F_{phr}^{(ab)}(n, T)$ (8) as functions of the height h of the solar atmosphere; (b) same as in (a) but for the parameter $F_{eei}^{(ab)}(n, T)$ (8).

2.2. Atmospheres of the DB White Dwarfs.

The chemi-ionization and chemi-recombination processes and consequently Rydberg atoms are of importance for cool stars and, first of all, for cool white dwarfs. Recently, a new effect has been noticed from Spitzer observations of cool white dwarfs [29]. Namely, these observations have demonstrated that some white dwarfs with $T < 6100 \text{ K}$ are found to display significant flux deficits in Spitzer observations (see [29]). These mid-IR flux deficits are not predicted by the current white dwarf models including collision induced absorption due to molecular hydrogen. This fact implies that the source of this flux deficit is not standard molecular absorption but some other physical process. It is possible that such process may be absorption by atoms and molecules in highly excited Rydberg states.

In the helium case of chemi-ionization and chemi-recombination processes, the situation turns out to be similar to the hydrogen case. This conclusion is based on the results obtained by Mihajlov and coworkers in [36]. The influence of symmetrical chemi-ionization and chemi-recombination processes on the helium atom Rydberg states population in weakly ionized layers of helium-rich DB white dwarfs has been investigated in [36].

Figure 6a,b show the obtained values of the total chemi-ionization and recombination rate coefficients $Kci(n, T)$ and $Kcr(n, T)$ in the region $3 \leq n \leq 10$ and $10,000 \text{ K} \leq T \leq 30,000 \text{ K}$ for helium plasma. The dependence of the both coefficients $Kci(n, T)$ and $Kcr(n, T)$ on the quantum number decreases with the increase of the temperature. Regarding the importance of the particular channel ('a' and 'b') for the chemi-ionization and chemi-recombination processes (1a,b), as can be seen in Figure 6b, conclusions are the same as for the chemi-ionization rate coefficients.

From the astrophysical viewpoint, chemi-ionization and chemi-recombination contribution to the Rydberg state populations have been compared with electron–electron–ion recombination, electron-excited atom ionization, and electron–ion photorecombination processes for n from 3 to 10, in helium-rich DB white dwarf atmosphere layers with logarithm of gravity $\log g = 7$ and 8 and effective temperature $T_{eff} \leq 20,000 \text{ K}$.

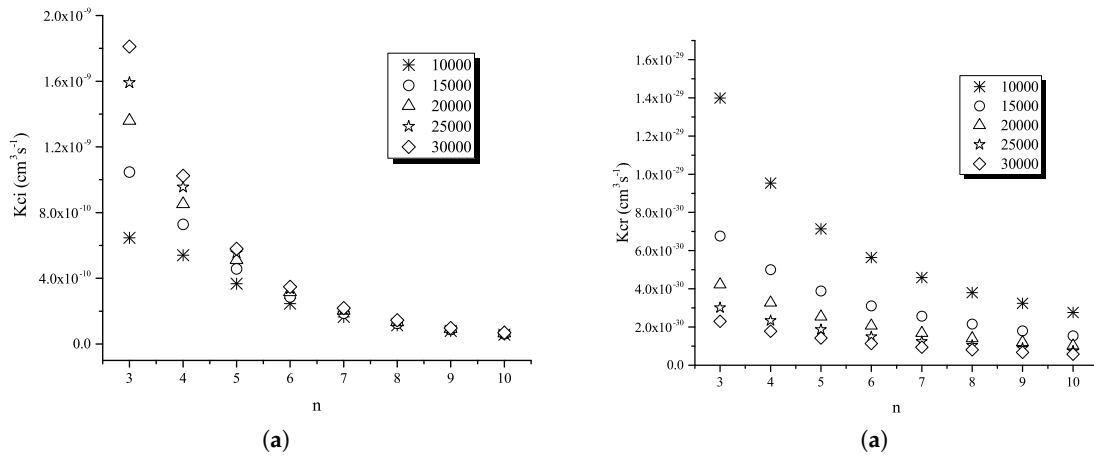


Figure 6. (a) total chemi-ionization rate coefficients $K_{ci}(n; T; \text{He})$ with $10,000 \text{ K} \leq T \leq 30,000 \text{ K}$ and for principal quantum numbers $n = 3-10$; (b) same as in (a) but for the inverse recombination coefficients $K_{cr}(n; T; \text{He})$ (data taken from [36]).

Some of the results obtained for the helium case [36] are illustrated by the Figure 7a,b, which are related to the recombination processes in the DB white dwarf atmosphere with an effective temperature $T_{\text{eff}} = 12,000 \text{ K}$. The values of the parameters $F_{\text{phr}}^{(ab)}(n, T)$ and $F_{\text{eei}}^{(ab)}(n, T)$ are given as functions of the logarithm of the Rosseland optical depth.

The results from [36] undoubtedly show that, for the lower temperatures, the chemi-ionization/recombination processes (1) are absolutely dominant over electron-excited atom ionization (3) and electron–electron–atom recombination (4) processes, for $n = 3, 4$, and 5 for almost all $\log \tau < 0$ values. For $n = 6, 7$, and 8 and in the same $\log \tau$ range, processes (1a,b) are comparable with processes (3) and (4). It is concluded that processes (1a,b) can be dominant ionization/recombination mechanisms in helium-rich DB white dwarf atmosphere layers for $\log g = 7$ and 8 and $T_{\text{eff}} \leq 20,000 \text{ K}$ and have to be implemented in relevant models of weakly ionized helium plasmas.

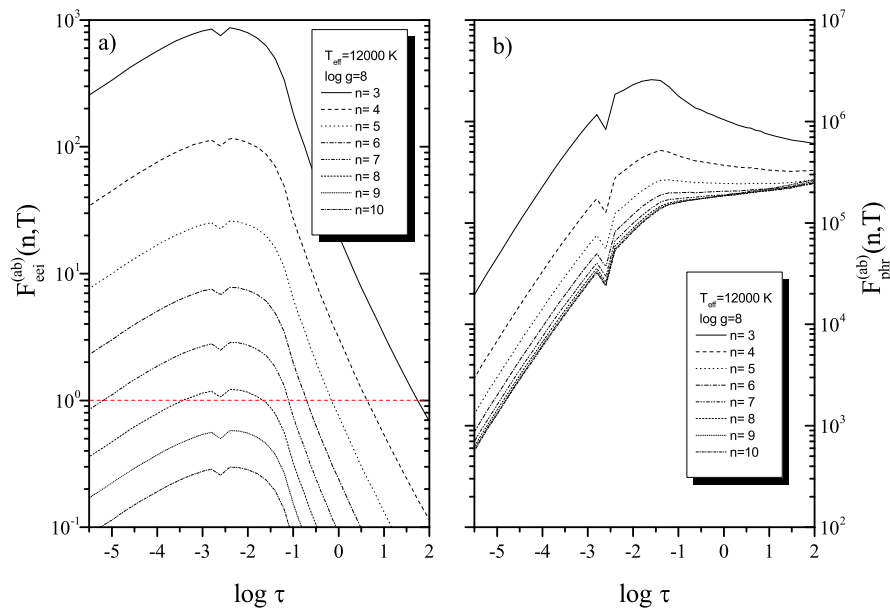
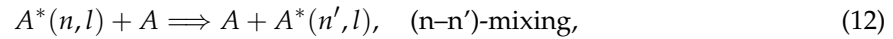


Figure 7. (a) parameter $F_{\text{eei}}^{(ab)}(n, T)$ (8) as a function of the logarithm of the Rosseland optical depth $\log \tau$; (b) as in (a) but for the parameter $F_{\text{phr}}^{(ab)}(n, T)$ (8).

2.3. Chemi-Ionization Processes in Solar and DB White-Dwarf Atmospheres in the Presence of Mixing Channels

In the recent paper of Mihajlov et al. [37], two kinds of atomic collision processes have been considered that simultaneously occur in the stellar atmospheres and influence each other (see Figure 8). This is about the chemi-ionization processes (1) and (n-n')-mixing i.e., excitation-deexcitation processes



where A are atoms in their ground states, $A^*(n, l)$ is an atom in a highly excited (Rydberg) state with the principal quantum number $n \gg 1$ and orbital quantum number l and $A = \text{H}$ or He .

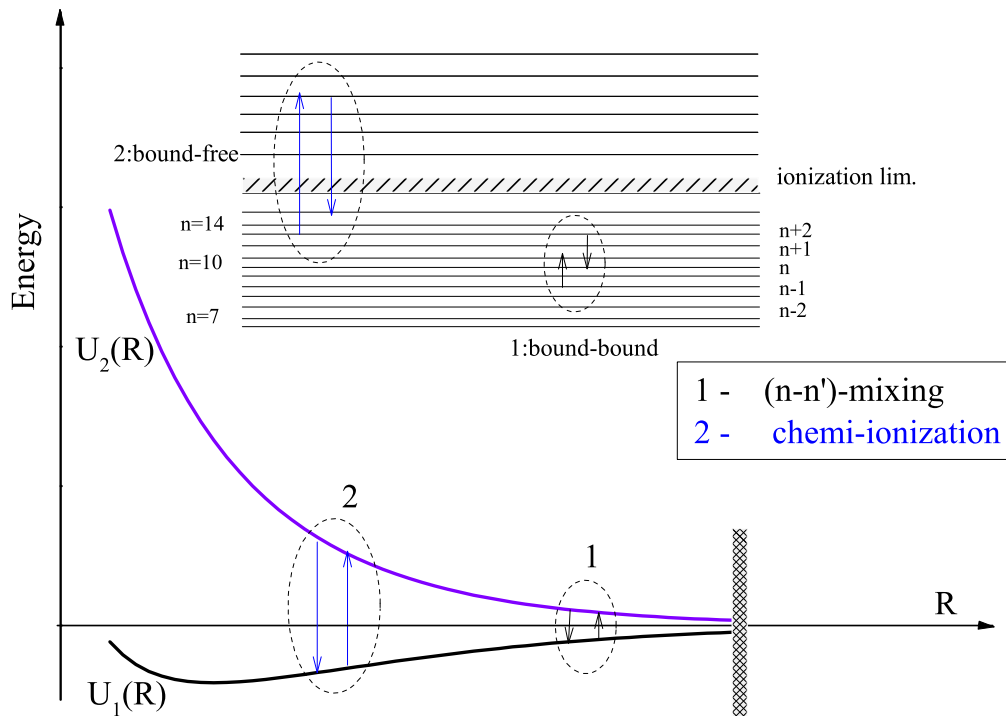


Figure 8. The schematic presentation of the chemi-ionization and (n-n')-mixing processes.

It was expected that process (12) would reduce the impact of chemi-ionization processes (1), as can be seen from the data of Mihajlov et al. (see Figure 9). The arrows in Figure 9a,b illustratively present that reduction of rate coefficients.

Mihajlov and coworkers have shown that, for the lower temperatures, the chemi-ionization processes are still dominant over electron-excited atom ionization processes ($A^*(n) + e \rightarrow A^+ + e + e$), for $n = 3, 4$, and 6 almost in the whole observed atmosphere which is illustrated by Figure 10 from [37]. For $n = 6, 7$, and 8 in the whole observed atmosphere, chemi-ionization processes are comparable with electron-excited atom ionization processes. This is illustrated in Figure 10a, for WD with $T_{eff} = 12,000$ K (helium case) and in Figure 10b for solar photosphere (hydrogen case).

From the results [37,38], it follows that processes (1) are significant for such hydrogen and helium plasmas with the ratio $Ne/Na < 10^{-3}$, where Ne and Na are the free electron and ground state atom density. Accordingly, these processes are significant for the stellar atmospheres that contain the corresponding weakly ionized layers.

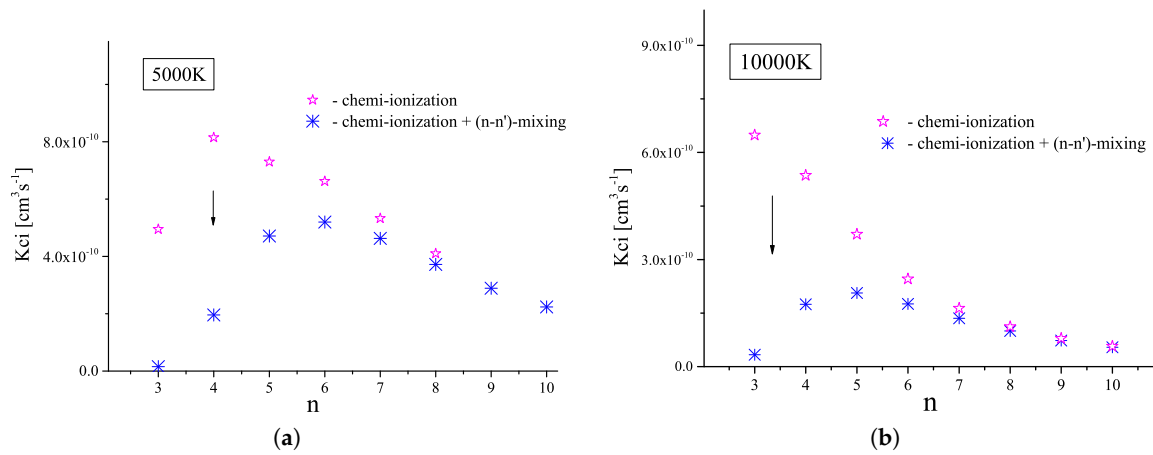


Figure 9. (a) comparison of the calculated values of rate coefficients of the chemi-ionization processes (1a,b) with and without inclusion of (n-n')-mixing process, case $A = H$; (b) same as in (a) but for case $A = He$.

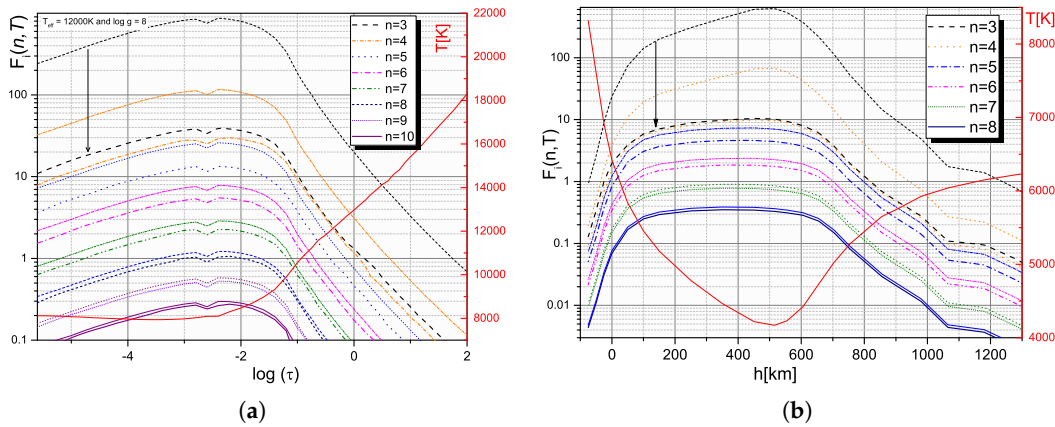


Figure 10. (a) parameter $F_i(n, T; He^*(n))$ (ratio of fluxes generated in atom–Rydberg–atom and electron-excited atom impact ionization) as a function of the logarithm of Rosseland optical depth $\log(\tau)$, for principal quantum numbers $n = 3-10$, with $T_{eff} = 12,000$ K and $\log g = 8$: wide line—present calculation; tiny line—calculation from [35]; (b) parameter $F_i(n, T; H^*(n))$ as a function of the height h , for principal quantum numbers $n = 3-8$, for model of solar photosphere [39]: wide line—present calculation; tiny line—calculation from [36].

2.4. The Atmospheres of Late Type Dwarfs (M Red Dwarfs)

The general stellar atmosphere code PHOENIX [10] has the advantage that, apart from solving the atmospheric structure, it also calculates output spectra. A good example of testing and application of PHOENIX code are processes (1) that influence the excited state populations and the free electron density, and also influence the atomic spectral line shapes.

In Reference [25], processes (1) are also considered in the case of an atmosphere of a M red dwarf with an effective temperature $T_{eff} = 3800$ K. The influence of these processes on the population of excited states of the hydrogen atom in this case was investigated using the PHOENIX code [10,16], which as a result generates a model of the considered atmosphere. In the framework of this work, the PHOENIX code includes processes (1) for $n \geq 4$. Some of the results obtained in [25] are illustrated by the Figure 11, where the values of the parameter ζ are presented, i.e., the ratio of the populations of the excited states of the hydrogen atom, calculated with and without taking into account processes (1). The presented figures show that, at least in the region $n \leq 15$, processes (1) equally affect the populations of the excited states of the hydrogen atom.

Then, Reference [25] shows that the processes (1) in the whole region of $n > 1$ also influence the free electron density (see Figure 12). This figure shows the behavior of free electron density calculated with these processes (solid curve) and without them (dashed curve).

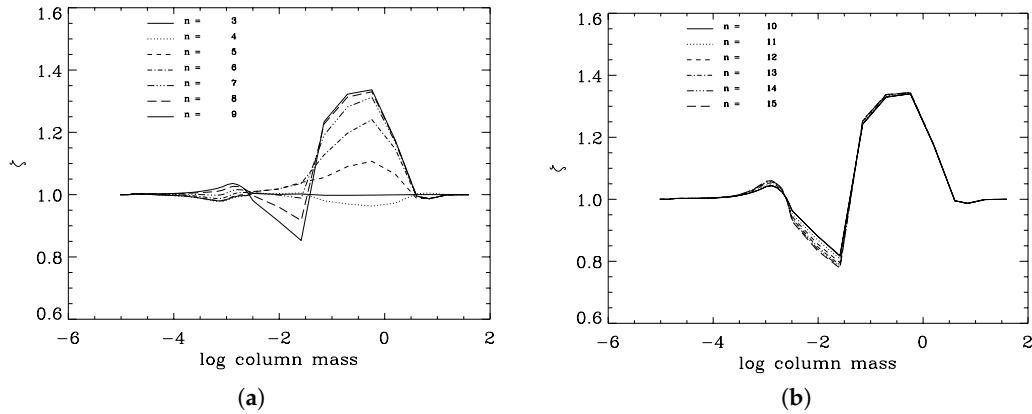


Figure 11. (a) the behavior of the population ratio ζ for $3 \leq n \leq 9$ as a function of the column mass; (b) same as in (a) but for $10 \leq n \leq 15$ (from [25]).

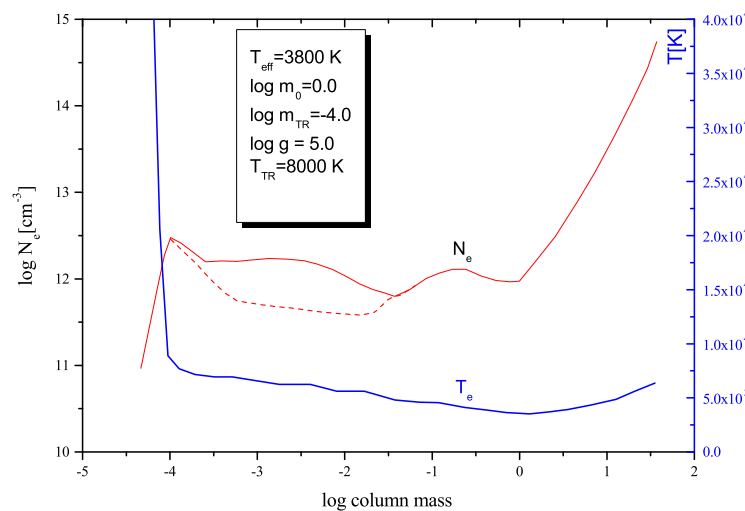


Figure 12. Structure of model atmosphere—electron density N_e and temperature T_e as a function of column mass.

The presented results suggested that processes (1), due to their influence on the excited state populations and the free electron density, also should influence the atomic spectral line shapes in the atmospheres of late type dwarfs.

2.5. Influences of Chemi-Ionization/Recombination Processes on the Hydrogen Spectral Lines in the M Red Dwarf Atmosphere

In connection with this problem, in Reference [26], the atmospheres of a M red dwarf with an effective temperature $T_{\text{eff}} = 3800 \text{ K}$ was also examined. In contrast to the previous case, processes (1) with $n = 2$ and 3 were included here.

The results presented in [26] show that the chemi-ionization/recombination processes (1), are directly affecting the population of the excited states of the hydrogen atom and the electron concentration, and thus have a very strong effect on the shape of the spectral lines of the atom. For the given atmosphere, the profiles of a number of spectral lines of the hydrogen atom were calculated.

Figure 13 (from [26]) show the line profiles of H_α , H_δ , H_ϵ Pa_ϵ with and without inclusion of processes (1). Profiles are synthesized with PHOENIX code with Stark broadening contribution calculated using tables from [40] for Stark broadening of hydrogen lines (linear Stark effect). Lineshape changes, especially in the wings, show the influence of the electron density change having a direct influence on the Stark broadening of hydrogen lines.

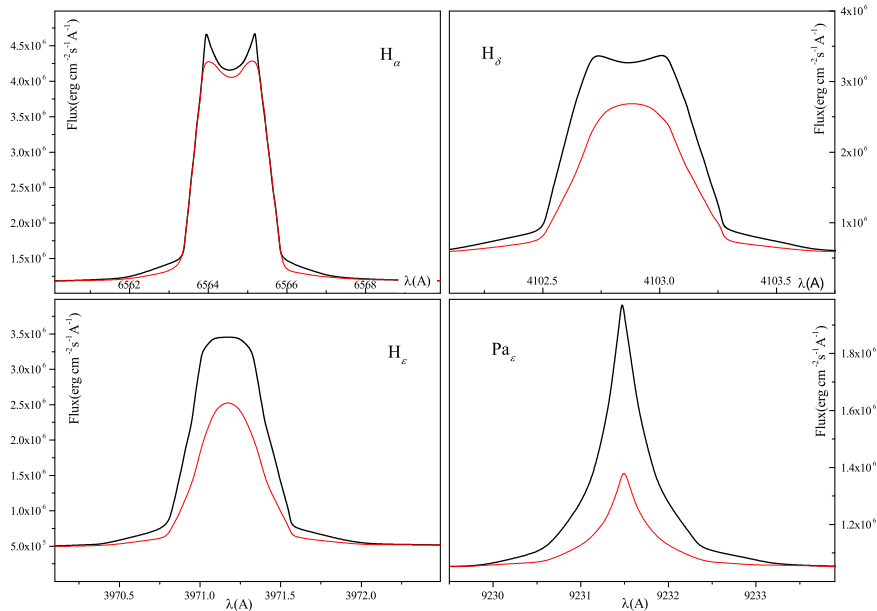


Figure 13. Line profiles with (full) and without (red tiny) inclusion of chemi-ionization and chemi-recombination processes for H lines.

3. Symmetric Ion–Atom Processes

It is well known [22] that the chemical composition of the primordial gas consists of electrons and species such as: helium—He, He^+ , He^{2+} and HeH^+ ; hydrogen—H, H^- , H^+ , H_2^+ and H_2 ; deuterium—D, D^+ , HD, HD^+ and HD^- ; lithium—Li, Li^+ , Li^- , LiH^- and LiH^+ . Evaluation of chemical abundances in the standard Big Bang model are calculated from a set of chemical reactions for the early universe [22]. Among them are very important reactions (2) that involve species like H, H^+ , H_2^+ , He^+ , He, He^+ , whose role in the primordial star formation is crucial.

Recently, References [41,42] have pointed out that the photodissociation of the diatomic molecular ion in the symmetric cases (2a) are of astrophysical relevance and could be important in modeling of specific stellar atmosphere layers, and they should be included in some chemical models. The data that involves reactions (2) are also useful in hydrogen and helium theoretical and laboratory plasmas research [43].

3.1. Solar Atmosphere: Visible Wavelength Region

The theoretical investigation of processes (2) started in [44] for the hydrogen symmetric case $A = H$. Then, in [44,45], the processes (2) were considered in relation to the photosphere and the lower solar chromosphere by characterizing their spectral emissivity $\epsilon_{ia}(\lambda)$, (the spectral density of the radiation energy, which these processes generate from a unit volume per unit time, into an angle 4π). Their contributions have been collated with concurrent processes (5)–(7) by comparative analysis of their influence using the values of the following parameters: $F_{ei}(\lambda) = \epsilon_{ia}(\lambda)/\epsilon_{ei}(\lambda)$, $F_{ea}^{ff}(\lambda) = \epsilon_{ia}(\lambda)/\epsilon_{ea}^{ff}(\lambda)$ and $F_{ea}^{fb}(\lambda) = \epsilon_{ia}(\lambda)/\epsilon_{ea}^{fb}(\lambda)$, where processes $\epsilon_{ei}(\lambda)$, $\epsilon_{ea}^{ff}(\lambda)$, and $\epsilon_{ea}^{fb}(\lambda)$ are their emissivity.

One of the major results obtained in papers of Mihajlov et al. [44,45] for the visible spectral region of the spectrum are illustrated by the Figure 14 for the considered layer of the solar atmosphere on the basis of standard models [39,46]. It was found that in this region processes (2) give a contribution of 10–12% in comparison with dominant processes (7). This fact alone demonstrated that considered ion–atom radiative processes must be taken into account for solar atmosphere modeling. Later estimates showed, however, that the relative influence of the absorption processes (2) on the solar atmosphere opacity should significantly increase at the transition from the considered wavelength region $\lambda \geq 365$ nm to the region $\lambda_H \leq \lambda < 365$ nm, where $\lambda_H = 91.1262$ nm is the wavelength that corresponds to the ionization threshold of the H(1s) atom.

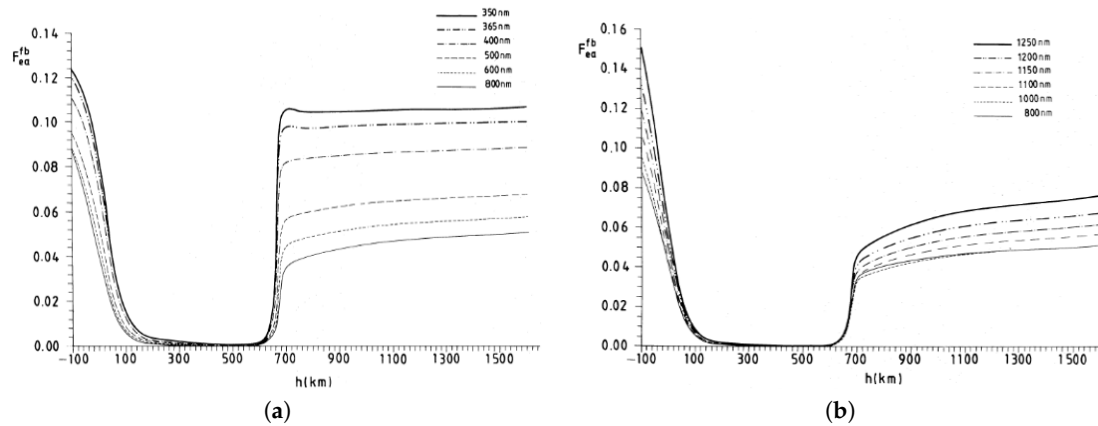


Figure 14. (a) the behaviour of the parameter $F_{ea}^{fb}(\lambda)$ as a functions of height h in the solar atmosphere for $350 \text{ nm} \leq \lambda \leq 800 \text{ nm}$; (b) the behaviour of the parameter $F_{ea}^{fb}(\lambda)$ as a function of height h of the solar atmosphere for $800 \text{ nm} \leq \lambda \leq 1250 \text{ nm}$ (from [44]).

3.2. Solar Atmosphere: UV and VUV Wavelength Region

In the far UV region, the emission channels of processes (2) cease to play a role, while the role of absorption channels in this region grows very rapidly. The total absorption rate coefficient $K_{ia} = K_{ia}^a + K_{ia}^b$ for processes (2a,b) as well as the branch coefficient $X = K_{ia}^b / K_{ia}$ which shows the influence of channels ‘a’ and ‘b’ in reaction (2) are presented in Figure 15a,b, respectively. The quantities K_{ia} and X are described in detail in [47] as well as their relations with cross sections. From Figure 15a one can see that K_{ia} strongly depends on temperature and wavelength and, from Figure 15b, it follows that, for lower temperatures, processes (2a) are dominant and importance of processes (2b) increases with the increase of temperature as expected.

In accordance with [47], in the Ultraviolet and Vacuum Ultraviolet regions, the influence of the absorption processes in processes (2) is estimated by the parameter, $F_k(\lambda)$ which is the ratio of the absorption coefficient of these processes and the absorption coefficient determined by the concurrent processes (5)–(7) taken together. The results obtained for the parameters $F_k(h)$ in the wavelength region $92 \text{ nm} \leq \lambda \leq 350 \text{ nm}$ are presented by Figure 16.

This figure shows that in the significant part of the considered region of altitudes ($-75 \text{ km} \leq h \leq 1065 \text{ km}$) the absorption processes (2) together give the contribution that varies from about 10% to about 90% of the contribution of the absorption processes (7), which are considered as the main absorption processes in the solar photosphere. In connection with the other known concurrent absorption processes, it is shown that, in the considered region of altitude, there are significant parts where the symmetric processes completely dominate (see also [48]).

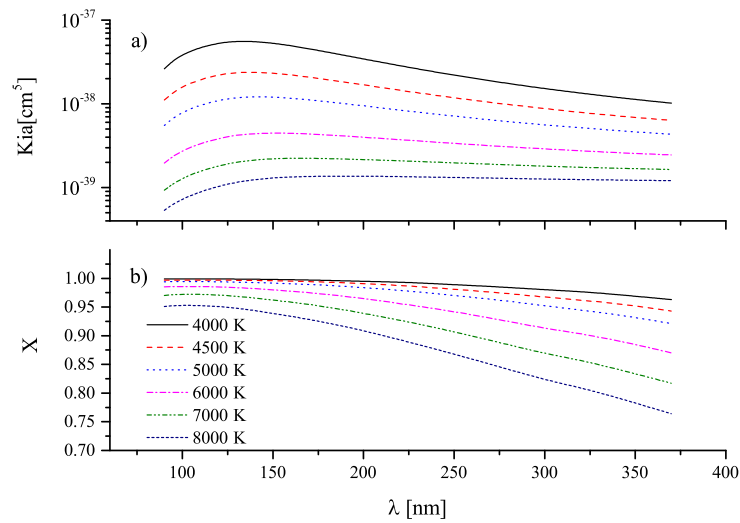


Figure 15. (a) the total absorption coefficient Kia as a function of λ and T ; (b) the branch coefficient X as a function of λ and T . Calculations from [47] case $A = H$.

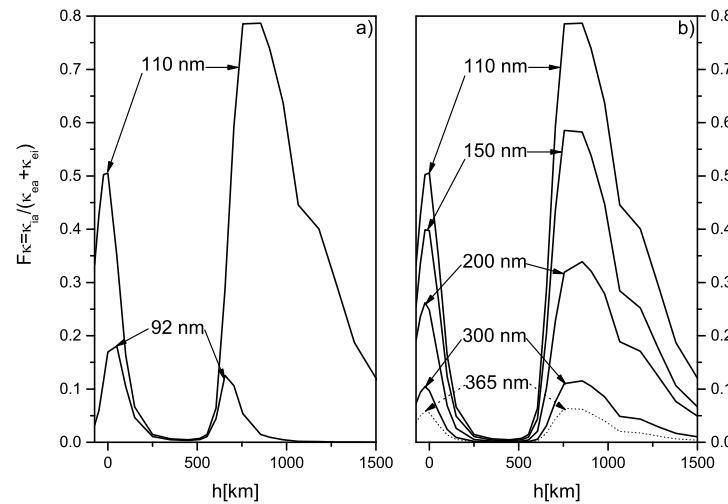


Figure 16. The behaviour of the parameter $F_k(\lambda)$ as a functions of height h in the solar atmosphere.

3.3. DB White Dwarf Atmospheres: Visible Wavelength Region

The results from [23], obtained for one Koester model ($\log g = 8$ and $T_{eff} = 12,000$ K), have already provided a more realistic picture of the relative importance of He^- (6) and He_2^+ (2a) total absorption processes, at least in the region $\lambda \leq 300$ nm. In a following paper [24], the relative importance of He_2^+ and other relevant absorption processes in the region $\lambda \geq 200$ nm was examined for several of Koester's (1980) models ($T_{eff} = 12,000, 14,000, 16,000$ K, $\log g = 7, 8$). It was shown that, in all considered cases, the contribution to opacity of the processes of He_2^+ molecular ion photodissociation and $He + He^+$ collisional absorption charge exchange combined is close to or at least comparable with the contribution of the absorption processes (6) and atomic absorption processes (5).

3.4. DB White Dwarf Atmospheres: UV and VUV Wavelength Region

Let us note in this context that, in the case of white dwarf atmospheres with dominant helium component, among all possible symmetric ion–atom absorption processes that are allowed by their composition, only the processes (2a,b) have to be taken into account [23,27].

Figure 17a presents the total absorption rate coefficient $K_{ia} = K_{ia}^a + K_{ia}^b$ for the processes (2a,b) as well as the branch coefficient $X = K_{ia}^b / K_{ia}$ that shows the influence of channels 'a' and 'b' in reaction (2). The quantities K_{ia} and X are described in detail in [27]. Regarding the importance of the particular channel ('a' and 'b') for the processes (2a,b), conclusions are the same as for the case of hydrogen.

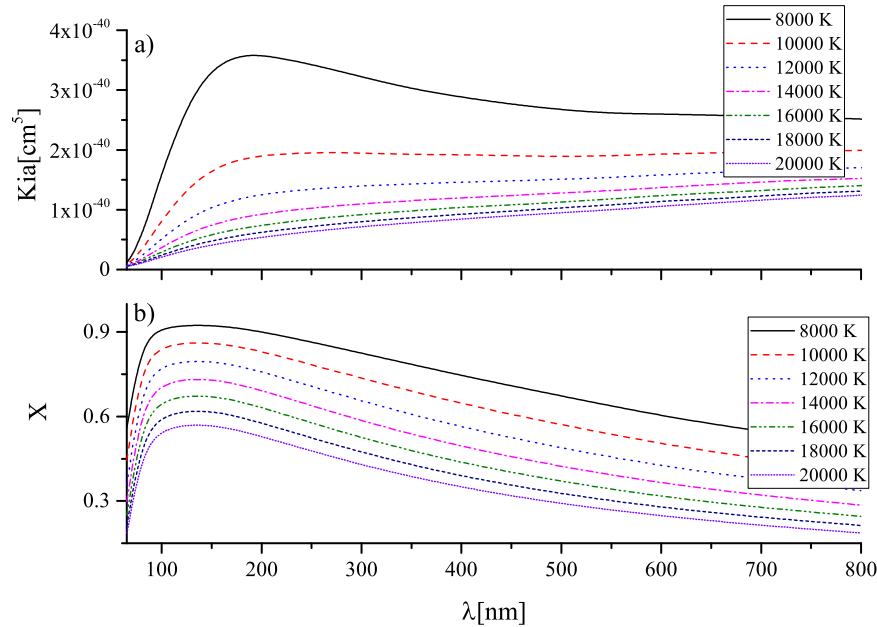


Figure 17. (a) the total absorption coefficient K_{ia} as a function of λ and T ; (b) the branch coefficient X as a function of λ and T . Data from [27], case $A = \text{He}$.

For the calculation of spectral properties, the data from the corresponding DB white-dwarf atmosphere models [49] have been used as well as the data for coefficients given in Figure 17. It was established that the processes (2a,b) significantly influence the opacity of the considered DB white dwarf atmospheres, with an effective temperature $T_{eff} \geq 12,000$ K, which fully justifies their inclusion in one of the models of such atmospheres [50]. However, the same comparison demonstrated also that the dominant role in those atmospheres generally still belongs to the concurrent absorption process (6), while the processes (2a,b) can be treated as dominant (with respect to this concurrent process) only in some layers of those atmospheres, and only within the part $50 \text{ nm} < \lambda < 250 \text{ nm}$ of the far UV and EUV region (see Figure 18). The results obtained in research allow for the possibility of estimating which absorption processes give the main contribution to the opacity in DB white dwarf atmospheres in different spectral regions. Therefore, from [23,27,51,52] results, it follows that the helium absorption processes (2a,b) are dominant in the region $70 \text{ nm} \leq \lambda \leq 200 \text{ nm}$, while, in the region $\lambda \geq 200 \text{ nm}$, the absorption processes (6) have an important role.

From the presented material, it follows that the considered symmetric ion–atom absorption processes cannot be treated only as one channel among many equal channels with influence on the opacity of the solar atmosphere. Namely, these symmetric processes around the temperature minimum increase the absorption of the EM radiation, so that this absorption becomes almost uniform in the whole solar photosphere

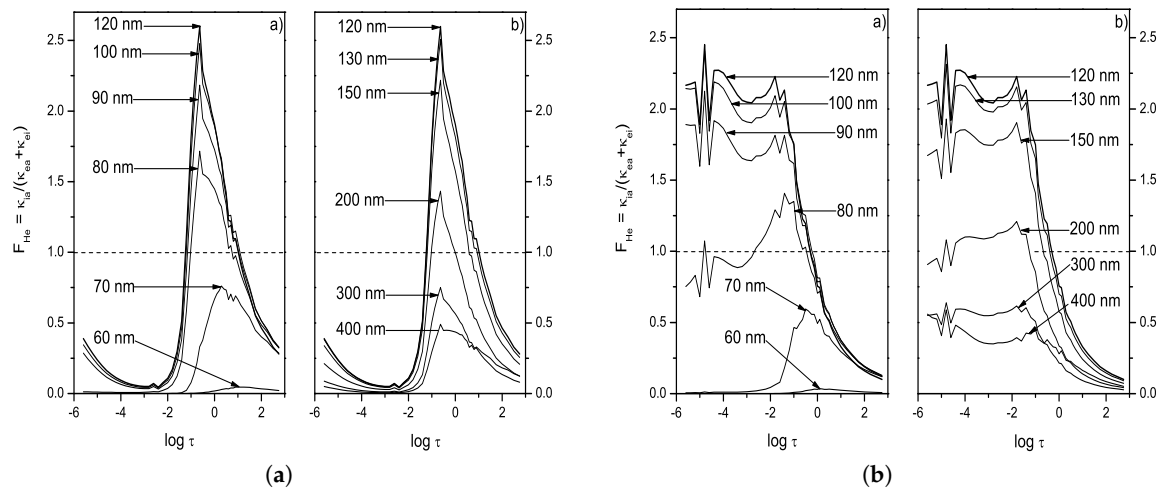


Figure 18. (a) behaviour of the quantity $F_{He} = \kappa_{ia} / (\kappa_{ea} + \kappa_{ei})$ (ratio of the absorption coefficients of processes (2), (5) and (6)) within the atmosphere of a DB white dwarf in the case $\log g = 8$ and $T_{eff} = 12,000$ K; (b) as in (a), but for the case $\log g = 8$ and $T_{eff} = 14,000$ K.

4. Conclusions

All the foregoing shows the undoubted influence of the radiation ion–atom processes and chemi-ionization/recombination processes on the optical properties and on the kinetics of weakly ionized layers of stellar atmospheres, and they should be studied from the spectroscopic aspect. In addition, it can be expected that the reported results will be a sufficient reason for including these processes in the models of stellar atmospheres. The further development of research in a new direction must be connected with the investigations of described processes but in the field of modelling in early Universe chemistry.

Acknowledgments: The authors are thankful to the Ministry of Education, Science and Technological Development of the Republic of Serbia for the support of this work within the projects 176002 and III44002.

Author Contributions: All authors contributed equally to this work.

Conflicts of Interest: The authors declare no conflict of interest.

References

1. Marinković, B.; Pejčev, V.; Filipović, D.; Šević, D.; Milosavljević, A.; Milosavljević, S.; Rabasović, M.; Pavlović, D.; Maljković, J. Cross section data for electron collisions in plasma physics. *J. Phys. Conf. Ser.* **2007**, *86*, 012006.
2. Marinković, B.P.; Jevremović, D.; Srećković, V.A.; Vujčić, V.; Ignjatović, L.M.; Dimitrijević, M.S.; Mason, N.J. BEAMDB and MolD—Databases for atomic and molecular collisional and radiative processes: Belgrade nodes of VAMDC. *Eur. Phys. J. D* **2017**, *71*, 158.
3. Srećković, V.A.; Ignjatović, L.M.; Jevremović, D.; Vujčić, V.; Dimitrijević, M.S. Radiative and Collisional Molecular Data and Virtual Laboratory Astrophysics. *Atoms* **2017**, *5*, 31.
4. Bezuglov, N.; Borodin, V.; Eckers, A.; Klyucharev, A. A quasi-classical description of the stochastic dynamics of a Rydberg electron in a diatomic quasi-molecular complex. *Opt. Spectrosc.* **2002**, *93*, 661–669.
5. Bezuglov, N.; Borodin, V.; Klyucharev, A.; Matveev, A. Stochastic dynamics of a Rydberg electron during a single atom–atom ionizing collision. *Russ. J. Phys. Chem.* **2002**, *76*, S27–S42.
6. Boyd, T.; Sanderson, J. *The Physics of Plasmas*; Cambridge University Press: Cambridge, UK, 2003.
7. Mason, N. The status of the database for plasma processing. *J. Phys. D* **2009**, *42*, 194003.
8. Campbell, L.; Brunger, M. Modelling of plasma processes in cometary and planetary atmospheres. *Plasma Sources Sci. Technol.* **2012**, *22*, 013002.

9. Larimian, S.; Lemell, C.; Stummer, V.; Geng, J.W.; Roither, S.; Kartashov, D.; Zhang, L.; Wang, M.X.; Gong, Q.; Peng, L.Y.; et al. Localizing high-lying Rydberg wave packets with two-color laser fields. *Phys. Rev. A* **2017**, *96*, 021403.
10. Hauschildt, P.; Baron, E. Cool stellar atmospheres with PHOENIX. *Mem. Soc. Astron. Ital.* **2005**, *7*, 140.
11. Christensen-Dalsgaard, J.; Dappen, W.; Ajukov, S.; Anderson, E.; Antia, H.M.; Basu, S.; Baturin, V.A.; Berthomieu, G.; Chaboyer, B.; Chitre, S.M.; et al. The current state of solar modeling. *Science* **1996**, *272*, 1286.
12. Fontenla, J.; Curdt, W.; Haberreiter, M.; Harder, J.; Tian, H. Semiempirical models of the solar atmosphere. III. Set of non-LTE models for far-ultraviolet/extreme-ultraviolet irradiance computation. *Astrophys. J.* **2009**, *707*, 482.
13. Kurucz, R.L. *Atlas: A Computer Program for Calculating Model Stellar Atmospheres*; SAO Special Report; Smithsonian Astrophysical Observatory: Cambridge, MA, USA, 1970; Volume 309.
14. Kurucz, R. *ATLAS9 Stellar Atmosphere Programs and 2 km/s Grid*; Kurucz CD-ROM No. 13; Smithsonian Astrophysical Observatory: Cambridge, MA, USA, 1993; Volume 13.
15. Gustafsson, B.; Bell, R.; Eriksson, K.; Nordlund, Å. A grid of model atmospheres for metal-deficient giant stars. I. *Astron. Astrophys.* **1975**, *42*, 407–432.
16. Hauschildt, P.H.; Baron, E. A 3D radiative transfer framework-VI. PHOENIX/3D example applications. *Astron. Astrophys.* **2010**, *509*, A36.
17. Husser, T.O.; Wende-von Berg, S.; Dreizler, S.; Homeier, D.; Reiners, A.; Barman, T.; Hauschildt, P.H. A new extensive library of PHOENIX stellar atmospheres and synthetic spectra. *Astron. Astrophys.* **2013**, *553*, A6.
18. Hubeny, I.; Hummer, D.; Lanz, T. NLTE model stellar atmospheres with line blanketing near the series limits. *Astron. Astrophys.* **1994**, *282*, 151–167.
19. Hubeny, I.; Lanz, T. Non-LTE line-blanketed model atmospheres of hot stars. 1: Hybrid complete linearization/accelerated lambda iteration method. *Astrophys. J.* **1995**, *439*, 875–904.
20. Hubeny, I.; Lanz, T. A brief introductory guide to TLUSTY and SYNSPEC. *arXiv* **2017**, arXiv:1706.01859.
21. Coppola, C.M.; Galli, D.; Palla, F.; Longo, S.; Chluba, J. Non-thermal photons and H₂ formation in the early Universe. *Mon. Not. R. Astron. Soc.* **2013**, *434*, 114–122.
22. Puy, D.; Dubrovich, V.; Lipovka, A.; Talbi, D.; Vonlanthen, P. Molecular fluorine chemistry in the early Universe. *Astron. Astrophys.* **2007**, *476*, 685–689.
23. Mihajlov, A.A.; Dimitrijevic, M.S.; Ignjatovic, L.M. The influence of ion–atom radiative collisions on the continuous optical spectra in helium-rich DB white-dwarf atmospheres. *Astron. Astrophys.* **1994**, *287*, 1026–1028.
24. Mihajlov, A.A.; Dimitrijević, M.S.; Ignjatović, L.M.; Djurić, Z. Radiative He⁺(1s) + He(1s²) Processes as the Source of the DB White Dwarf Atmosphere Electromagnetic Continuous Spectra. *Astrophys. J.* **1995**, *454*, 420.
25. Mihajlov, A.A.; Jevremović, D.; Hauschildt, P.; Dimitrijević, M.S.; Ignjatović, L.M.; Alard, F. Influence of chemi-ionization and chemi-recombination processes on the population of hydrogen Rydberg states in atmospheres of late type dwarfs. *Astron. Astrophys.* **2003**, *403*, 787–791.
26. Mihajlov, A.A.; Jevremović, D.; Hauschildt, P.; Dimitrijević, M.S.; Ignjatović, L.M.; Alard, F. Influence of chemi-ionization and chemi-recombination processes on hydrogen line shapes in M dwarfs. *Astron. Astrophys.* **2007**, *471*, 671–673.
27. Ignjatović, L.M.; Mihajlov, A.A.; Sakan, N.M.; Dimitrijević, M.S.; Metropoulos, A. The total and relative contribution of the relevant absorption processes to the opacity of DB white dwarf atmospheres in the UV and VUV regions. *Mon. Not. R. Astron. Soc.* **2009**, *396*, 2201–2210.
28. Mihajlov, A.A.; Srećković, V.A.; Ignjatović, L.M.; Klyucharev, A.N. The Chemi-Ionization Processes in Slow Collisions of Rydberg Atoms with Ground State Atoms: Mechanism and Applications. *J. Clust. Sci.* **2012**, *23*, 47–75.
29. Kilić, M.; von Hippel, T.; Mullally, F.; Reach, W.; Kuchner, M.; Winget, D.; Burrows, A. The mystery deepens: Spitzer observations of cool white dwarfs. *Astrophys. J.* **2006**, *642*, 1051.
30. Gnedin, Y.N.; Mihajlov, A.A.; Ignjatović, L.M.; Sakan, N.M.; Srećković, V.A.; Zakharov, M.Y.; Bezuglov, N.N.; Klyucharev, A.N. Rydberg atoms in astrophysics. *New Astron. Rev.* **2009**, *53*, 259–265.
31. O’Keeffe, P.; Bolognesi, P.; Avaldi, L.; Moise, A.; Richter, R.; Mihajlov, A.A.; Srećković, V.A.; Ignjatović, L.M. Experimental and theoretical study of the chemi-ionization in thermal collisions of Ne Rydberg atoms. *Phys. Rev. A* **2012**, *85*, 052705.

32. Lin, C.; Gocke, C.; Röpke, G.; Reinholz, H. Transition rates for a Rydberg atom surrounded by a plasma. *Phys. Rev. A* **2016**, *93*, 042711.
33. Mihajlov, A.A.; Dimitrijević, M.S.; Djurić, Z. Rate coefficients of collisional $H-H^+(n)$ ionization and $H-H^+-e$ and H_2^+-e recombination. *Phys. Scr.* **1996**, *53*, 159–166.
34. Mihajlov, A.A.; Ignjatović, L.M.; Vasiljević, M.M.; Dimitrijević, M.S. Processes of $H-H^+-e$ and H_2^+-e recombination in the weakly-ionized layers of the solar atmosphere. *Astron. Astrophys.* **1997**, *324*, 1206–1210.
35. Mihajlov, A.A.; Ignjatović, L.M.; Srećković, V.A.; Dimitrijević, M.S. Chemi-ionization in Solar Photosphere: Influence on the Hydrogen Atom Excited States Population. *Astrophys. J. Suppl. Ser.* **2011**, *193*, 2.
36. Mihajlov, A.; Ignjatović, L.M.; Dimitrijević, M.; Djurić, Z. Symmetrical chemi-ionization and chemi-recombination processes in low-temperature layers of helium-rich DB white dwarf atmospheres. *Astrophys. J. Suppl. Ser.* **2003**, *147*, 369.
37. Mihajlov, A.A.; Srećković, V.A.; Ignjatović, L.M.; Dimitrijević, M.S. Atom-Rydberg-atom chemi-ionization processes in solar and DB white-dwarf atmospheres in the presence of $(n-n')$ -mixing channels. *Mon. Not. R. Astron. Soc.* **2016**, *458*, 2215–2220.
38. Mihajlov, A.A.; Srećković, V.A.; Ignjatović, L.M.; Klyucharev, A.N.; Dimitrijević, M.S.; Sakan, N.M. Non-Elastic Processes in Atom Rydberg-Atom Collisions: Review of State of Art and Problems. *J. Astrophys. Astron.* **2015**, *36*, 623–634.
39. Vernazza, J.E.; Avrett, E.H.; Loeser, R. Structure of the solar chromosphere. III - Models of the EUV brightness components of the quiet-sun. *Astrophys. J. Suppl. Ser.* **1981**, *45*, 635–725.
40. Vidal, C.R.; Cooper, J.; Smith, E.W. Unified theory calculations of Stark broadened hydrogen lines including lower state interactions. *J. Quant. Spectrosc. Radiat. Transf.* **1971**, *11*, 263–281.
41. Babb, J.F. State resolved data for radiative association of H and H^+ and for Photodissociation of H_2^+ . *Astrophys. J. Suppl. Ser.* **2015**, *216*, 21.
42. Heays, A.; Bosman, A.; van Dishoeck, E. Photodissociation and photoionisation of atoms and molecules of astrophysical interest. *Astron. Astrophys.* **2017**, *602*, A105.
43. Dubernet, M.; Antony, B.; Ba, Y.; Babikov, Y.L.; Bartschat, K.; Boudon, V.; Braams, B.; Chung, H.K.; Daniel, F.; Delahaye, F.; et al. The virtual atomic and molecular data centre (VAMDC) consortium. *J. Phys. B* **2016**, *49*, 074003.
44. Mihajlov, A.A.; Dimitrijević, M.S.; Ignjatović, L.M. The contribution of ion-atom radiative collisions to the opacity of the solar atmosphere. *Astron. Astrophys.* **1993**, *276*, 187.
45. Mihajlov, A.A.; Dimitrijević, M.; Ignjatović, L.; Djurić, Z. Spectral coefficients of emission and absorption due to ion-atom radiation collisions in the solar atmosphere. *Astron. Astrophys. Suppl. Ser.* **1994**, *103*.
46. Maltby, P.; Avrett, E.; Carlsson, M.; Kjeldseth-Moe, O.; Kurucz, R.; Loeser, R. A new sunspot umbral model and its variation with the solar cycle. *Astrophys. J.* **1986**, *306*, 284–303.
47. Mihajlov, A.; Ignjatović, L.M.; Sakan, N.; Dimitrijević, M. The influence of H_2^+ -photo-dissociation and $(H + H^+)$ -radiative collisions on the solar atmosphere opacity in UV and VUV regions. *Astron. Astrophys.* **2007**, *469*, 749–754.
48. Srećković, V.A.; Mihajlov, A.A.; Ignjatović, L.M.; Dimitrijević, M.S. Ion-atom radiative processes in the solar atmosphere: Quiet Sun and sunspots. *Adv. Space Res.* **2014**, *54*, 1264–1271.
49. Koester, D. Model atmospheres for DB white dwarfs. *Astron. Astrophys. Suppl. Ser.* **1980**, *39*, 401–409.
50. Bergeron, P.; Wesemael, F.; Beauchamp, A. Photometric calibration of hydrogen and helium rich white dwarf models. *Publ. Astron. Soc. Pac.* **1995**, *107*, 1047.
51. Ignjatović, L.M.; Mihajlov, A.A.; Srećković, V.A.; Dimitrijević, M.S. Absorption non-symmetric ion-atom processes in helium-rich white dwarf atmospheres. *Mon. Not. R. Astron. Soc.* **2014**, *439*, 2342–2350.
52. Mihajlov, A.A.; Ignjatović, L.M.; Srećković, V.A.; Dimitrijević, M.S.; Metropoulos, A. The non-symmetric ion-atom radiative processes in the stellar atmospheres. *Mon. Not. R. Astron. Soc.* **2013**, *431*, 589–599.

